Nuclear Instruments and Methods in Physics Research B 267 (2009) 377–381

Contents lists available at ScienceDirect

Nuclear Instruments and Methods in Physics Research B

journal homepage: www.elsevier.com/locate/nimb

Electron transport coefficients in N_2O in RF electric and magnetic fields

Olivera Šašić [a,b,*], Snježana Dupljanin [a,c], Saša Dujko [a], Zoran Lj. Petrović [a]

[a] Institute of Physics, POB 68, 11080 Belgrade, Serbia
[b] Faculty for Traffic and Transport Engineering, University of Belgrade, Vojvode Stepe 305, 11000 Belgrade, Serbia
[c] Phys. Dept., Faculty of Science, M. Stojanovića 2, Banjaluka, Bosnia and Herzegovina

ARTICLE INFO

Available online 17 October 2008

PACS:
34.80.-i
51.10.+y
52.80.Pi
52.65.-y

Keywords:
Transport coefficients
Monte Carlo
N_2O
RF fields

ABSTRACT

A Monte Carlo simulation technique is used to investigate electron transport in N_2O in crossed RF electric and magnetic fields. Our work has resulted in a database of transport parameters which can be used for correct implementation in modeling RF discharges. A behavior of transport coefficients under the influence of the magnitude and the frequency of the fields was studied separately revealing some complex features in the time dependence, most notably anomalous anisotropic diffusion and time-resolved negative differential conductivity.

1. Introduction

Nitrous-oxide (N_2O), as an electronegative gas, is widely applicable in chemistry, medicine (as an anesthetic) and technology, in particular for the N doping of oxide materials [1], and deposition of diamond-like carbon films [2]. Furthermore, it has a significant impact on environment as it causes the damage to the ozone layer, and has an influence on the infrared absorption in the atmosphere [3,4]. Even so, it has been suggested as a potential replacement to gases which have an even higher global warming potential, but are still used as gas insulators (such as SF_6). That is why it seems reasonable to put additional effort in finding efficient way for decomposing this biogenic gas. More specifically atmospheric pressure discharges that are required for numerous applications are often produced in RF fields to maintain their non-equilibrium character. Thus it is at least needed to understand transport of electrons in those gases in RF fields in order to put together reliable models.

Because of its great importance, N_2O was studied on numerous occasions. In spite of that, there is a lack of reliable and complete sets of both electron transport and collision data. Some discrepancies between existing data, even for the case of constant electric field are noticeable while electron kinetics in the presence of a magnetic field, or in the case of time varying electric and magnetic fields, has not been studied yet. This is a critical point for modeling of processes leading to further optimization of low-temperature RF plasma applications [5–7]. Due to the lack of available transport data in RF fields and, on the other hand, because of their complexity that make them difficult to be included in both fluid and hybrid codes, the only available option for modeling RF plasmas was the extrapolation of the electron transport properties obtained in dc electric field. Typical examples include the application of the so-called quasi-static approximation for the low field frequencies and/or the effective field approximation for higher field frequencies. However, both of these approximations fail for the range of frequencies critical for any practical applications in plasma processing. In addition, in the majority of previous works in plasma modeling community the effect of a magnetic field usually is not taken into account at all. This contrasts with the modern day demands for rigorous models of plasma discharges, where magnetic fields sometimes play a vital role in device behavior. With these remarks as a background, we approach the problem at two stages: initially, in this work, we focus on electron kinetics in time dependent electric and magnetic fields and defer the detailed consideration of the electron transport and collision data to a future but more comprehensive paper [8]. Therefore, primary aim of this paper is to check what kind of kinetic phenomena in electron transport in N_2O may be expected to occur and how are those related to the cross sections.

2. Monte Carlo simulation technique

We have used our time-resolved Monte Carlo simulation code that has been described in great detail in some of our previous

* Corresponding author. Address: Institute of Physics, POB 68, 11080 Belgrade, Serbia.
E-mail address: o.sasic@sf.bg.ac.yu (O. Šašić).

0168-583X/$ - see front matter © 2008 Elsevier B.V. All rights reserved.
doi:10.1016/j.nimb.2008.10.025

publications [9–12]. The code has been verified for a number of benchmarks [9,10] which prove its correctness and numerical integrity. In our simulation we have followed the evolution of 5×10^5 of initial electrons through time and an infinite space, under the influence of spatially uniform and time dependent crossed electric and magnetic fields, with the phase difference of $\pi/2$ rad. The number of initial electrons was chosen carefully in order to achieve a good statistics of the output data and still to have reasonable duration of the simulations. Initial velocity distribution function was Maxwellian with the mean starting energy of 1 eV. The density of neutrals was 3.54×10^{22} m^{-3} which corresponded to the gas pressure of 1 Torr (133.3 Pa), at 273 K. As calculation was for sufficiently high mean energies and thus not affected by the choice of gas temperature it was assumed to be 0 K. Swarm conditions are assumed to apply and mutual interaction between electrons is negligible compared with electron–molecule interactions. In other words, our calculations were made for the low density limit of the gas discharge as is the standard procedure in determination of transport coefficients for non-equilibrium plasmas [13–15].

The exact moment of electron–molecule collision was determined by solving the equation for collision probability:

$$p(t) = \nu_T(\varepsilon(t)) \exp\left(-\int_{t_0}^{t} \nu_T(\varepsilon(t'))dt'\right),$$

where $\nu_T(\varepsilon)$ is the total collision frequency, t_0 is either the time of the electron entering into gas or the time of a previous collision and ε is the electron energy. This equation is solved by numerical integration in small time steps which can be determined as the minimum of the following relevant time constants: period of the fields, mean collisional time and cyclotron period for $E \times B$ fields. The period of the field is always divided by 100 and these segments are used to sample the basic dynamic electron properties such as position, velocity, energy, etc. After relaxation to a quasi-stationary state (or relaxed periodic state), the results may be presented over a single period of the field but usually we have averaged the results over many periods in order to obtain better statistics. The definitions and formulae for electron transport coefficients were given in our previous publications [10,11]. All electron scattering were assumed to be isotropic regardless of the nature of collisions. The elastic and inelastic collisions were included in a complete (n terms of number, momentum and energy balances) set of cross sections. The most reliable data were taken from the literature [16–18]. In our analysis [8] the data were renormalized in order to fit the most recent experimental results for the drift velocities and effective ionization coefficients [19]. The improved set of cross sections employed in this work is shown in Fig. 1.

3. Results and discussion

3.1. Time dependence of transport coefficients as a function of B/N

In this section we discuss the basic features of the time dependence of transport coefficients for different values of reduced magnetic field (B/N). We have performed a series of simulations using the following set of input parameters: the gas pressure was 1 Torr, the field frequency was set to 100 MHz (that, due to ω/N scaling, correspond to the pressure of 100 mTorr and field frequency of 10 MHz which is typical for many applications), the reduced electric field of 100 Td (1 Td = 10^{-21} Vm^2) and the range of the reduced magnetic fields given by their amplitude as 0, 200, 500, 1000, 2000 Hx (1 Hx = 10^{-27} Tm^3) were used.

In Fig. 2 we show the temporal profiles of the mean energy as a function of phase for different B/N. As can be seen, the mean energy is reduced as the amplitude of B/N increases. At the same time the profile of the mean energy at the highest B/N considered in this work becomes asymmetric and triangular with a fast increase and a slower decrease.

Fig. 3 shows the temporal profiles of the longitudinal component of the drift velocity (W_E) as a function of phase for different B/N. For lower B/N the peak is wide and smooth, centered around zero magnetic field and its magnitude is almost unaffected by the presence of the field. For an increasing of B/N it becomes narrow and its phase is shifted.

As expected, the perpendicular component along the $E \times B$ direction ($W_{E\times B}$) increases with B/N (see Fig. 4). Its shape changes from sinusoidal to saw tooth profile and becomes clearly asymmetric. When the magnetic field goes through its zero value, strong electric field allows electrons to accelerate and gain energy, longitudinal component of drift velocity reaches its peak while the perpendicular component goes through a quick fall. After that the latter one rises much slower and some oscillations become visible in both cases. It can also be seen that $W_{\mathbf{E}\times\mathbf{B}}$ has a non-zero mean value which causes the rotational macroscopic motion of electron swarm.

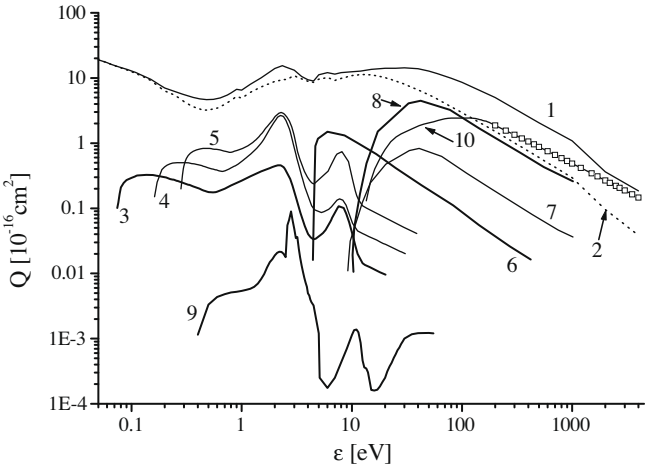

Fig. 1. Electron impact cross sections for electrons in N_2O used in this study. Cross sections in the figure are 1 – total momentum transfer, 2 – elastic momentum transfer, 3, 4, 5 – vibrational excitation, 6, 7, 8 – electronic excitation, 9 – dissociative attachment, 10 – ionization (open symbols represent extrapolation).

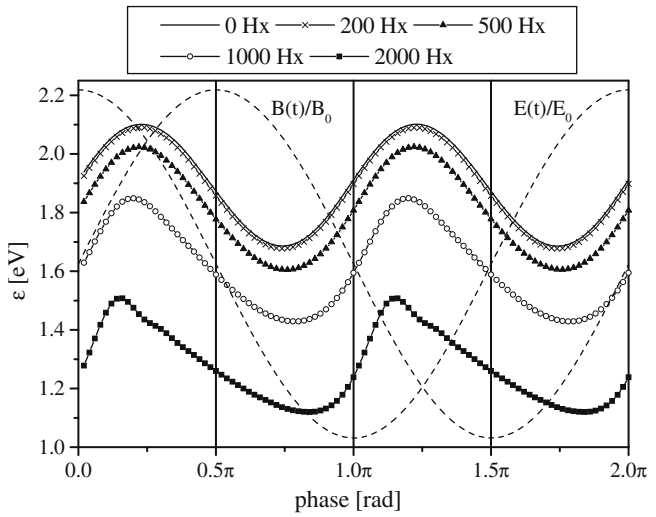

Fig. 2. Temporal profiles of the mean energy as a function of B/N. The frequency of the field is 100 MH and E/N = 100 Td.

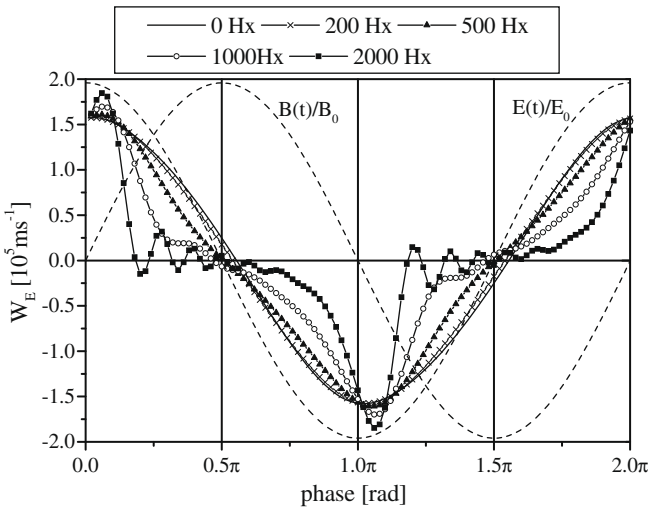

Fig. 3. Time dependence of the drift velocity component along the direction of the electric field for different values of B/N, at E/N = 100 Td and f = 100 MHz.

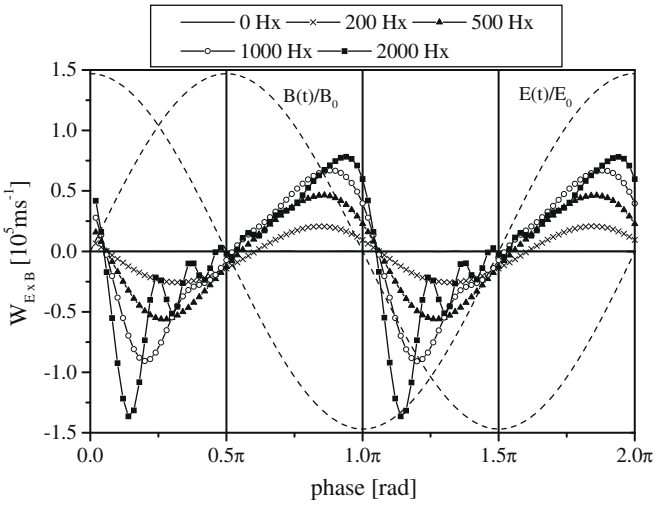

Fig. 4. Time dependence of the drift velocity component along the $E \times B$ direction, for different values of B/N, at E/N = 100 Td and f = 100 MHz.

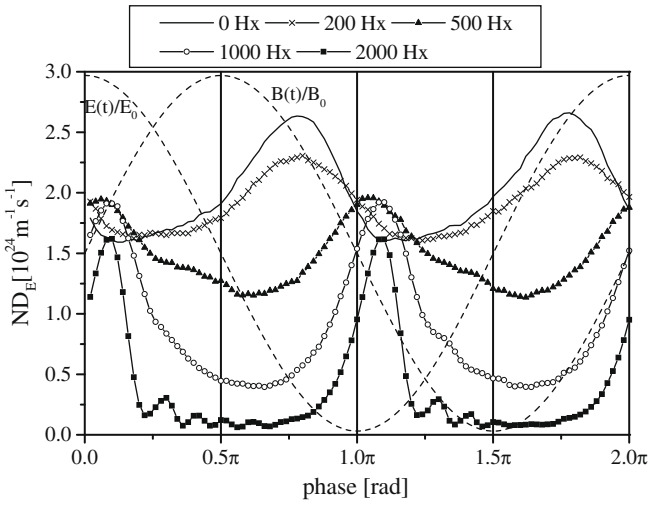

Fig. 5. Temporal profiles of the longitudinal diffusion coefficient (ND_E) as a function of B/N, at E/N = 100 Td and f = 100 MHz.

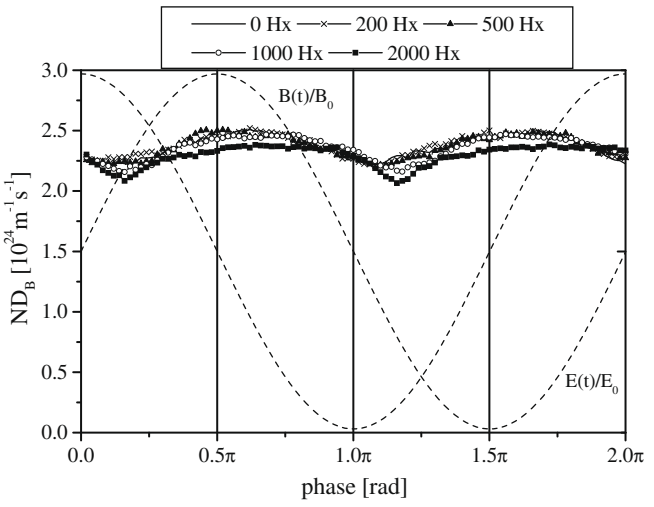

Fig. 6. Temporal profiles of the transverse diffusion coefficient along the direction of the magnetic field (ND_B) as a functions of B/N at E/N = 100 Td and f = 100 MHz.

As expected, when B/N increases, the longitudinal component of diffusion tensor (ND_E) decreases (see Fig. 5) due to a joint decrease in both the longitudinal drift velocity component and mean energy. Peaks are shifted to the phase of strong electric field, more in tune with the W_E peaks (Fig. 3) and at the highest B/N diffusion is significantly reduced for all other phases. In contrast to ND_E, the transverse diffusion coefficient along B direction (ND_B) is not much affected by the magnetic field (see Fig. 6). Only small modulations can be observed and minor reduction at the peak values which is consistent with the results for the Reid ramp model [12].

Behavior of the $E \times B$ component of the diffusion tensor ($ND_{E\times B}$) is presented in Fig. 7. We observe that this transport quantity is a decreasing function of B/N. It is interesting to note that $ND_{E\times B}$ peaks for phases when the electric field has its maximum value. The position of these peaks are not affected by the action of magnetic field and in the limit of the highest B/N considered here. $ND_{E\times B}$ begins to behave like the ND_E component of the diffusion tensor. Perhaps the most striking property associated with the diffusion tensor is the presence of 'negative' diffusion in $ND_{E\times B}$. This negative excursion appears at those phases of the field where the electric field is low in magnitude and for the highest B/N of 2000 Hx. The reader is referred to [20] where the phenomenon of negative diffusion is explained in great detail.

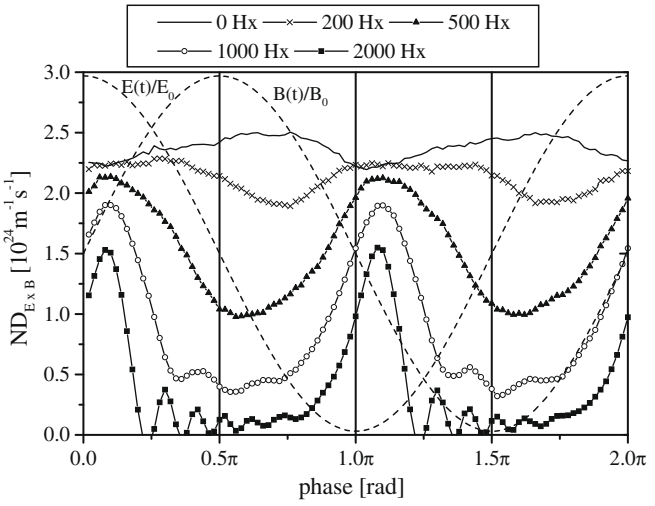

Fig. 7. Temporal profiles of the transverse diffusion coefficient along the $E \times B$ direction ($ND_{E\times B}$) as a function of B/N at E/N = 100 Td and f = 100 MHz.

3.2. Time dependence of transport coefficients as a function of the frequency of the field

We show the basic features of the time dependence of transport coefficients as a function of the electric field frequency (f). In order to obtain these results we performed MC simulation at E/N = 100 Td, B/N = 0 Hx, f = 10, 50, 100, 500, 1000 MHz, with the same concentration of neutrals as in the previous case.

In Fig. 8 we show the temporal profiles of the drift velocity as a function of the field frequency. One can observe signs of the time-resolved negative differential conductivity (NDC) [21] for the field frequency of 10 MHz. If the field frequency increases, the shape of the time dependence changes to sinusoidal while modulation is decreased. In the limit of the highest frequency of 1 GHz, the profile is sinusoidal with the phase shift of $\pi/2$ to the electric field which is a clear sign that electrons undergo many oscillations per collision. On average the electric field can no longer pump energy into the system and transport approaches the thermal limit.

Fig. 9 illustrates the effect of anomalous behavior of the longitudinal diffusion (ND_L) coefficient in RF fields. The anomaly is reflected in the following. First, ND_L peaks during or just after the phases when the electric field changes the sign. Second, for a brief period of phase period, ND_L becomes larger than the transverse diffusion coefficient (ND_T). In DC fields, however, the diffusion is anisotropic and $ND_T > ND_L$ holds for the similar energy range. This phenomenon was observed for a range of model and real gases and explained in some of previous publications [10,22,23].

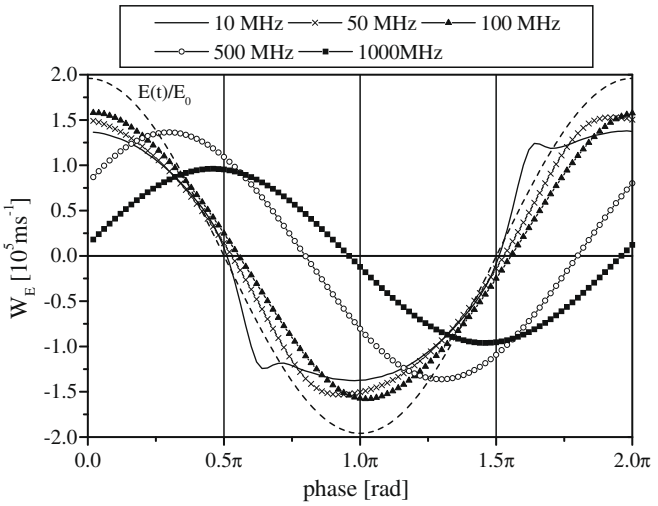

Fig. 8. Temporal profiles of the drift velocity as a function of the field frequency at E/N = 100 Td and B/N = 0 Hx.

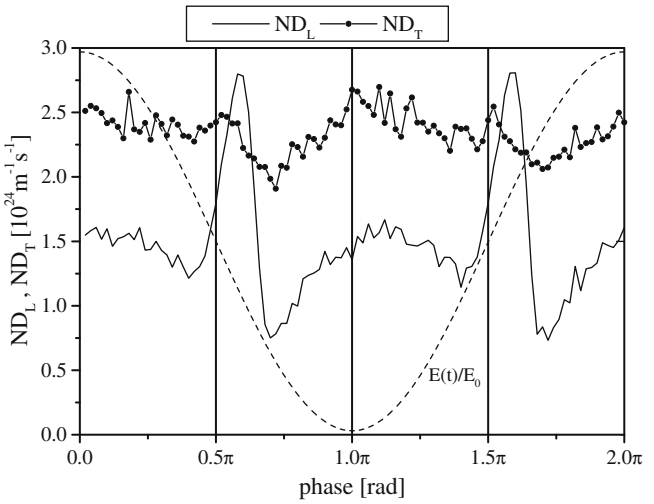

Fig. 9. Time dependence of the transverse (ND_T) and longitudinal (ND_L) diffusion coefficients at E/N = 100 Td, B/N = 0 Hx and f = 10 MHz.

4. Conclusion

Using a Monte Carlo simulation technique the electron transport in time dependent electric and magnetic fields is examined under conditions that are critical for plasma modeling. In particular, the mean energy, drift velocity and diffusion tensor components are studied under the influence of the magnetic field strengths and field frequencies. The presented data, together with the accurate set of cross sections [8], are required to model non-equilibrium plasmas and plasma devices.

Our investigation revealed that electron transport coefficients are strongly affected by the presence of the magnetic field. The mean energy of electron swarm decreases as B/N increases. The time dependence of the perpendicular component of the drift velocity is modified to saw tooth profile inducing asymmetry in its profile. A behavior of the longitudinal component of the drift velocity and diffusion coefficients is in agreement with the predictions based on the results associated with previous investigation of electron kinetics for certain model gases [10]. The effect of the frequency of electric field was studied and discussed separately.

The most interesting features in the time dependencies of the electron transport coefficients found within this investigation include the following: the signs of time-resolved negative differential conductivity associated with the drift velocity, the transiently negative diffusivity associated with the $E \times B$ component of the diffusion tensor and anomalous behavior of the longitudinal diffusion coefficient. One must consider these phenomena, at least in order to check whether plasma codes may be able to predict the occurrence some of these phenomena when they are applied to N_2O containing plasmas.

Acknowledgements

Authors are grateful to J. de Urquijo, T.D. Märk and T. Makabe for useful suggestions and providing us with data. This work was performed under Project 141025 of the Ministry of Science of Serbia.

References

[1] H. Matsui, H. Saeki, K. Tomoji, H. Tabata, B. Mizobuchi, J. Appl. Phys. 95 (2004) 5882.
[2] Y.T. Kim, S.G. Yoon, S.G. Yoon, S.C. Yung, S.J. Suh, D.H. Yoon, Surf. Coat. Technol. 180–181 (2004) 250.
[3] P. Crutzen, J. Geophys. Res. 76 (1971) 7311.
[4] T.E. Graedel, P.J. Crutzen, Atmospheric Change: An Earth System Prospective, Freeman, New York, 1993.
[5] M.J. Kushner, J. Appl. Phys. 58 (1985) 4024.
[6] N. Nakano, N. Shimura, Z.Lj. Petrović, T. Makabe, Phys. Rev. E 49 (1994) 4455.
[7] E. Shidoji, K. Ness, T. Makabe, Vacuum 60 (2001) 299.
[8] S. Dupljanin, O. Šašić, J. de Urquijo, Z.Lj. Petrović, et al. (in preparation).
[9] S. Bzenić, Z.M. Raspopović, S. Sakadžić, Z.Lj. Petrović, IEEE Trans. Plasma Sci. 27 (1999) 78.
[10] Z.Lj. Petrović, Z.M. Raspopović, S. Dujko, T. Makabe, Appl. Surf. Sci. 192 (2002) 1.
[11] S. Dujko, Z.M. Raspopović, Z.Lj. Petrović, J. Phys. D: Appl. Phys. 38 (2005) 2952.
[12] Z.M. Raspopović, S. Sakadžić, Z.Lj. Petrović, T. Makabe, J. Phys. D: Appl. Phys. 33 (2000) 1298.
[13] Z.Lj. Petrović, M. Šuvakov, Ž. Nikitović, S. Dujko, O Šašić, J. Jovanović, G. Malović, V. Stojanović, Plasma Sources Sci. Technol. 16 (2007) S1.
[14] R.E. Robson, R.D. White, Z.Lj. Petrović, Rev. Mod. Phys. 77 (2005) 1303.
[15] L.G.H. Huxley, R.W. Crompton, The Diffusion and Drifts of Electrons in Gases, Wiley, New York, 1974.

[16] J. Mechlińska-Drewko, T. Wróblewski, Z.Lj. Petrović, V. Novaković, G.P. Karwasz, Rad. Phys. Chem. 68 (2003) 205.
[17] E. Märk, T.D. Märk, Y.B. Kim, K. Stephan, J. Chem. Phys. 75 (1981) 4446.
[18] <http://www.rjd.web.cern.ch/rjd/cgi-bin/cross?update>.
[19] E. Basurto, J.L. Hernández-Avila, A.M. Juárey, J. de Urquijo, S. Dupljanin, O. Šašić, Z.Lj. Petrović, in: 28th ICPIG, 15–20 July 2007, Prague, Czech Republic, p. 227.
[20] R. D White, S. Dujko, K.F. Ness, R E Robson, Z. Raspopović, Z.Lj. Petrović, J. Phys. D: Appl. Phys. 41 (2008) 025206.
[21] S. Bzenić, Z. Lj. Petrović, Z.M. Raspopović, T. Makabe, Jpn. J. Appl. Phys. 38 (1999) 6077.
[22] R.D. White, R.E. Robson, K.F. Ness, Aust. J. Phys. 48 (1995) 925.
[23] K. Maeda, T. Makabe, N. Nakano, S. Bzenić, Z.Lj. Petrović, Phys. Rev. E 55 (1997) 5901.